The Astrophysical Journal, 921:120 (7pp), 2021 November 10 https://doi.org/10.3847/1538-4357/ac25eb

An Eclipsing Black Widow Pulsar in NGC 6712

Zhen Yan[1,2,3], Zhi-chen Pan[2,4,5], Scott M. Ransom[6], Duncan R. Lorimer[7,8], Lei Qian[4,5], Pei Wang[4,5], Zhi-qiang Shen[1,2,3], Di Li[4,2,9], Peng Jiang[2,4,5], Jin-Tao Luo[2,10], Jie Liu[1,2], and Zhi-peng Huang[1,2]
[1] Shanghai Astronomical Observatory, Chinese Academy of Sciences, NO. 80 Nandan Road, Shanghai 200030, People's Republic of China; yanzhen@shao.ac.cn
[2] University of Chinese Academy of Sciences, No.19A Yuquan Road, Shijingshan District, Beijing 100049, People's Republic of China
[3] Key Laboratory of Radio Astronomy, Chinese Academy of Sciences, 10 Yuanhua Road, Nanjing, JiangSu 210033, People's Republic of China
[4] National Astronomical Observatories, Chinese Academy of Sciences, 20A Datun Road, Chaoyang District, Beijing 100101, People's Republic of China
[5] CAS Key Laboratory of FAST, National Astronomical Observatories, Chinese Academy of Sciences, Beijing 100101, People's Republic of China
[6] National Radio Astronomy Observatory, Charlottesville, VA 22903, USA
[7] Department of Physics and Astronomy, West Virginia University, Morgantown, WV 26506, USA
[8] Center for Gravitational Waves and Cosmology, West Virginia University, Chestnut Ridge Research Building, Morgantown, WV 26505, USA
[9] NAOC-UKZN Computational Astrophysics Centre, University of KwaZulu-Natal, Durban 4000, South Africa
[10] National Time Service Center, Chinese Academy of Sciences, Xi'an 710600, People's Republic of China
Received 2020 November 24; revised 2021 September 2; accepted 2021 September 9; published 2021 November 8

Abstract

We report the discovery of the first radio pulsar associated with NGC 6712, an eclipsing black widow (BW) pulsar, J1853–0842A, found by high-sensitivity searches using the Five-hundred-meter Aperture Spherical radio Telescope. This 2.15 ms pulsar is in a 3.56 hr compact circular orbit with a very low mass companion likely of mass 0.018 to 0.036 $M_\odot$ and exhibits eclipsing of the pulsar signal. Though the distance to PSR J1853–0842A predicted from its dispersion measure ($155.125 \pm 0.004\,\mathrm{cm^{-3}\,pc}$) and Galactic free electron density models are about 30% smaller than that of NGC 6712 obtained from interstellar reddening measurements, this is likely due to limited knowledge about the spiral arms and Scutum stellar cloud in this direction. Follow-up timing observations spanning 445 days allow us to localize the pulsar's position to be 0.14 core radii from the center of NGC 6712 and measure a negative spin-down rate for this pulsar of $-2.39(2) \times 10^{-21}\,\mathrm{s\,s^{-1}}$. The latter cannot be explained without the acceleration of the globular cluster (GC) and decisively supports the association between PSR J1853–0842A and NGC 6712. Considering the maximum GC acceleration, the Galactic acceleration, and the Shklovskii effect, we place an upper limit on the intrinsic spin-down rate to be $1.11 \times 10^{-20}\,\mathrm{s\,s^{-1}}$. From an analysis of the eclipsing observations, we estimate the electron density of the eclipse region to be about $1.88 \times 10^6\,\mathrm{cm^{-3}}$. We also place an upper limit of the accretion rate from the companion at about $3.05 \times 10^{-13}\,M_\odot\,\mathrm{yr^{-1}}$, which is comparable with some other BWs.

Unified Astronomy Thesaurus concepts: Pulsars (1306)

1. Introduction

Globular clusters (GCs) are tightly bound by gravity, giving them spherical shapes and relatively high stellar densities toward their centers. This environment provides a high specific incidence of low-mass X-ray binaries (LMXBs), the proposed progenitors of millisecond pulsars (MSPs), which enhances the possibility of finding new pulsars in GCs compared to the Galactic disk (see, e.g., Pooley et al. 2003; Ransom 2008). Since the discovery of the first pulsar in M28 (Lyne et al. 1987), there are currently about 217 pulsars known to be associated with Galactic GCs, most of these are binary MSPs (Freire 2013).[11] In the core of a GC, more frequent interactions between stars take place as the stellar densities get even higher. The stellar interactions also produce exotic MSP binaries that are extremely rare in other places. The MSP is thought to have been spun up by the transfer of matter and angular momentum from its low-mass companion star during an X-ray-emitting phase. When a neutron star has been spun up to millisecond periods, its strong radiation has a possibility of quenching accretion by ablating surrounding plasma, potentially evaporating the companion entirely to form an isolated MSP (Ruderman et al. 1989). Support for this scenario is provided by discoveries of eclipsing redback (RB; Archibald et al. 2009) and black widow (BW; Fruchter et al. 1988) pulsars. These systems typically have compact orbits with periods shorter than 24 hr and are accompanied by low-mass companions with typical masses a few tenths of a solar mass or less ($<0.1\,M_\odot$ for BWs and 0.2–0.4 $M_\odot$ for RBs). Evolutionary studies of BWs and RBs can provide important links between LMXBs and MSPs (Roberts 2013).

According to the catalog of GCs in the Milky Way, NGC 6712 is a metal-rich GC located about 6.9 kpc away from the Sun. The core and half-light radii of NGC 6712 are 0′.76 and 1′.33, respectively. In Table 1, we list useful properties of NGC 6712 related to this work obtained from the catalog[12] of GCs (Harris 1996). The stellar encounter rate for a GC can be estimated with $\Gamma \propto \rho_c^{1.5} r_c^2$, where ρ_c and r_c are the density and radius of the cluster core, respectively (Verbunt & Hut 1987). For NGC 6712, Γ is less than 1% of Terzan 5, where 39 pulsars have been discovered. In NGC 6712, there is an LMXB with an orbital period (P_b) of 0.33 hr detected with the Einstein Observatory's Monitor Proportional Counter (Leahy et al. 1983). In spite of a number of radio pulsar

[11] http://www3.mpifr-bonn.mpg.de/staff/pfreire/GCpsr.html

[12] http://physwww.mcmaster.ca/~harris/mwgc.dat

Table 1
Observed Properties of NGC 6712

Name	NGC 6712
R.A. (J2000)	$18^h53^m04\overset{s}{.}3$
Decl. (J2000)	$-08°42'22\overset{''}{.}0$
Galactic longitude, l, (deg)	25.35
Galactic latitude, b, (deg)	−4.32
Distance, D, (kpc)	6.9
Core radius, r_c, (arcmin)	0.76
Half-light radius, r_h, (arcmin)	1.33
Central velocity dispersion, σ_v (km s^{-1})	4.3

searches in NGC 6712 previously carried out, prior to this work, no pulsars were known in this cluster. This led to upper limits on pulsed emission of 11 mJy at 400 MHz (Biggs & Lyne 1996) and 16 μJy at 2.0 GHz (Lynch et al. 2011). Using scaling laws derived in previous population studies, which show that Γ is a strong indicator of pulsar abundance in GCs (Hui et al. 2010; Turk & Lorimer 2013), we estimate the population of pulsars in NGC 6712 to be ∼5—much smaller than Terzan 5 and highlighting the importance of sensitive surveys such as the work described in this paper.

The Five-hundred-meter Aperture Spherical radio Telescope (FAST) is the largest single-dish radio telescope in the world (Nan 2006; Nan et al. 2011; Qian et al. 2020). Benefiting from its 300 m illuminated aperture and low-noise cryogenic receivers, FAST can perform unprecedented high-sensitivity observations (Jiang et al. 2019). In this paper, we will present pulsar search results of NGC 6712 with FAST that have led to the discovery of the first pulsar in this cluster, PSR J1853–0842A. The rest of this paper is structured as follows: in Section 2, we describe the observations and data reduction procedures; in Section 3, we present the results of the search and follow-up timing observations; and in Section 4, we discuss the implications and significance of our results.

2. Observations and Data Reduction

Observations of NGC 6712 were carried out with FAST using the central beam of the 19-beam L-band receiver (Jiang et al. 2020). For these observations, where the typical system temperature is about 20 K, the unparalleled gain of FAST leads to a system-equivalent flux density of about 2 Jy, at least a factor of 3 improvement over the previous observations mentioned above. To carry out a dispersion measure (DM) search, the total bandwidth (1.05−1.45 GHz) was divided into subchannels of 0.12 MHz and the data were acquired using the pulsar searching mode with a time resolution of 49.152 μs. Following our discovery of the pulsar in the initial 30 minute observation carried out on 2019 June 25 (MJD 58,659), confirmation and follow-up observations were arranged on MJDs 58,685 (observation length $T_o = 120$ min, T_o will be omitted hereafter), 58,686 (60 minutes), 58,687 (30 minutes), 58,768 (30 minutes), 58,769 (30 minutes), 58,931 (60 minutes), 58,933 (60 minutes), 58,963 (10 minutes), 58,965 (10 minutes), and 59,105 (30 minutes).

All data were searched for the presence of periodic dispersed pulses using the PulsaR Exploration and Search TOolkit (PRESTO[13]; Ransom 2011). Within PRESTO, the routine rfifind was used to mask and zap radio-frequency interference in both the time and frequency domains. The predicted DM of NGC 6712 is about 182 cm^{-3} pc based on its distance (6.9 kpc; Harris 1996) and the YMW16 Galactic free electron density models (Yao et al. 2017). As no pulsar was discovered in NGC 6712 previously, we searched for periodic signals in a DM range 0–300 pc cm^{-3} with a step of 0.05 pc cm^{-3}. The PRESTO routine accelsearch was used to analyze the data using a Fourier-domain acceleration search technique (Ransom et al. 2002), which, for a spin frequency f and an observation length T, was sensitive to frequency drifts $z = \dot{f}T^2$ of up to $z_{max} = 200$ Fourier bins. To search for even more highly accelerated binary systems, we also used the so-called "jerk search" technique (Andersen & Ransom 2018) that looks for signal drifts $w = \dot{z} = \ddot{f}T^3$. In our searches, we set the maximum drift $w_{max} = 600$ bins. The python script ACCEL_sift.py was used to produce a winnowed list of pulsar candidates from the searches. Besides the periodic pulse signal, we also used single_pulse_search.py to search for single pulses by setting the threshold to be 5.0.

3. Results

We found a promising pulsar candidate with a spin period $P = 2.149$ ms and DM of 155.13 cm^{-3} pc in the initial observation from MJD 58,659. With jerk search, the signal-to-noise ratios (S/Ns) of candidate detection was enhanced from 44.06 to 45.97. The signal was subsequently redetected in follow-up observations with an S/N in the range 20.26–48.39. Each detection of the pulsar was further refined using the PRESTO routine prepfold, which searched the data in period and DM to produce integrated pulse profiles with subintegration lengths of 1.2 minutes. These period searches provided P and $\dot{P}$ measurements for each observation that were then used to obtain a preliminary estimate of the orbital parameters of the pulsar using the analysis technique described by Freire et al. (2001). This initial spin and orbital ephemeris was subsequently supplied as input to the TEMPO[14] software package (Nice et al. 2015), which we used to carry out a full phase-coherent timing analysis of the time of arrival (TOA) for each folded profile. We used the get_toa.py routine in PRESTO (which is an implementation of Fourier-domain template matching; Taylor 1992) to obtain TOAs that were analyzed in TEMPO using well-established methods (Lorimer & Kramer 2004).

The timing analysis resulted in a phase-coherent solution for the new pulsar, which we henceforth refer to as PSR J1853–0842A, over the MJD range 58,659–59,105. The timing residuals as a function of MJD, TOA number, and orbital phase are presented in Figure 1. The measured and derived parameters of PSR J1853–0842A are listed in Table 2. As seen in Figure 1, the extra time delays take place on three separate days, all of which correspond to the same orbital phase range (0.22–0.32). These phenomena should be caused by the eclipse of ionized material surrounding the companion star, as dispersion time delay was detected if we divided the total bandwidth into two subbands with the central frequencies of 1.15 and 1.35 GHz, respectively. The emission from the MSP is ablating its companion in such a narrow binary orbit. Assuming the eclipsing material to be spherically symmetric and centered in the orbital plane at the distance of the companion, the maximum extra time delay is expected when

[13] https://www.cv.nrao.edu/~sransom/presto

[14] http://tempo.sourceforge.net

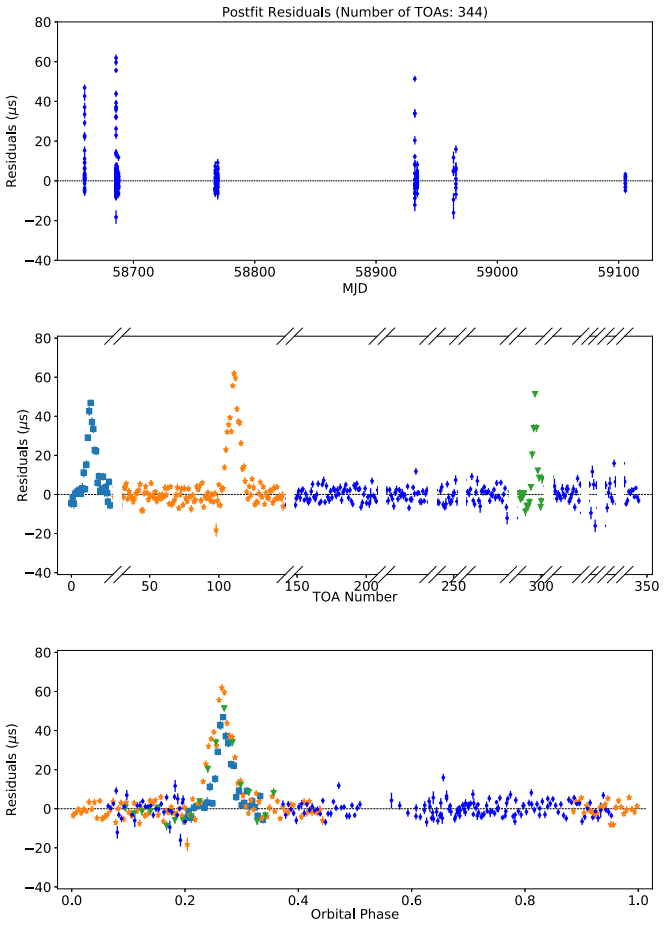

Figure 1. Timing residuals for PSR J1853–0842A as a function of MJD (top), time-of-arrival (TOA) number (middle), and orbital phase (bottom). The cyan squares, orange stars, and green triangles in the plot shown in the middle and bottom panels correspond to the observation results on MJD 58,659, 58,685, and 58,931, respectively. Pulsar eclipses were detected on each of these days. In the middle panel, observation results from different epochs are separated by breaks on the horizontal axes of the plot. The integration length of each point is about 1.2 minutes.

the companion passes closest to our line of sight toward the pulsar (Polzin et al. 2019).

In Figure 2, we present two samples of phase–time and integrated profile plots for PSR J1853–0842A based on the observations from MJD 58,685 and 58,768. The subintegration time for the phase–time plots is about 7 minutes. Obvious time delays caused by the eclipse are detected around 4900 s in the phase–time plot of observation on MJD 58,685. The integrated profile of PSR J1853–0842A shows a simple structure with only a single peak. The widths at 50% and 10% of the peak of the integrated profile are $W_{50} = 26.^{\circ}04 \pm 1.^{\circ}24$ and $W_{10} = 63.^{\circ}41 \pm 2.^{\circ}56$, respectively.

Since there were no radio flux density calibrators arranged in our observations, we estimate the flux density of PSR J1853–0842A using radiometer noise calculations (see, e.g., Lynch et al. 2011), which gives the off-pulse rms noise,

$$\sigma = \frac{T_{\rm sys}}{G\sqrt{N_p \Delta\nu T_{\rm o}}}. \quad (1)$$

Here $T_{\rm sys}$, G, N_p, $\Delta\nu$, and $T_{\rm o}$ are the system noise temperature, antenna gain, number of polarization, bandwidth, and length of observation, respectively. Using the nominal values for these parameters, and adopting $G = 11.3\ {\rm K\ Jy^{-1}}$ (Jiang et al. 2019), since the zenith angle is large in our observations, we find the estimated mean flux density of PSR J1853–0842A to be $16.1 \pm 2.9\ \mu Jy$ at 1.25 GHz.

Table 2
Observed and Derived Parameters of PSR J1853–0842A

Pulsar	J1853–0842A
R.A., α (J2000)	$18^h53^m04.^s07409(2)$
Decl., δ (J2000)	$-08^{\circ}42'28.''254(2)$
Spin Frequency, f_0 (s^{-1})	465.23897161363(7)
1st Spin Frequency derivative, f_1 (Hz s^{-2})	$5.18(4) \times 10^{-16}$
Reference Epoch (MJD)	58,685.702931
Start of Timing Data (MJD)	58,659.715
End of Timing Data (MJD)	59,105.545
Dispersion Measure, DM (pc cm^{-3})	155.125(4)
Solar System Ephemeris	DE200
Number of TOAs	344
Residuals rms (μs)	3.77
Binary Parameters	
Binary Model	BT
Projected Semimajor Axis, x_p (lt-s)	$4.91856(2) \times 10^{-2}$
Orbital Eccentricity, e	0.00
Longitude of Periastron, ω (deg)	0.00
Epoch of passage at Periastron, T_0 (MJD)	58,685.64161943(9)
Orbital Period, P_b (days)	0.1482829972(2)
Derived Parameters	
Spin Period, P (s)	$2.1494330032835(3) \times 10^{-3}$
1st Spin Period derivative, $\dot{P}$ ($s\ s^{-1}$)	$-2.39(2) \times 10^{-21}$
Distance based on TC93[a], $D_{\rm TC93}$ (kpc)	4.55
Distance based on NE2001[b], $D_{\rm NE2001}$ (kpc)	3.79
Distance based on YMW16[c], $D_{\rm YMW16}$ (kpc)	4.76
Mass function, $f(M_p, M_c)$ ($M_\odot$)	5.81×10^{-6}
Possible range of M_c[d] ($M_\odot$),	$0.018 \leqslant M_c \leqslant 0.036$

Notes.
[a] Taylor & Cordes (1993).
[b] Cordes & Lazio (2002).
[c] Yao et al. (2017).
[d] For $i \geqslant 60.^{\circ}0$ and $1.0\ M_\odot \leqslant M_p \leqslant 2.2\ M_\odot$ (see Section 4).

4. Discussion

Besides the 6.9 kpc adopted in the Galactic GC catalog (Harris 1996), there are some other distance results of NGC 6712, e.g., 6.75 kpc (Sandage & Smith 1966), 6.2 kpc (Webbink 1985), and 7.9 kpc (Ortolani et al. 2000), that were also obtained base on interstellar reddening measurements. Overall, DM-based distances of PSR J1853–0842A listed in Table 1 are much smaller than previous distance results of NGC 6712. Normally, distance results obtained with interstellar reddening measurements are comparatively reliable, as they are supported by model-independent parallax measurements on a large sample of stars at the optical band (Fuhrmann 2004). By comparison, only 144 pulsars' distances are obtained with parallax measurements.[15] To further investigate PSR J1853–0842A is in NGC 6712 or not, we first used constraints from Galactic electron density models along this line of sight. Comparisons of model-independent distances of

[15] http://hosting.astro.cornell.edu/~shami/psrvlb/parallax.html

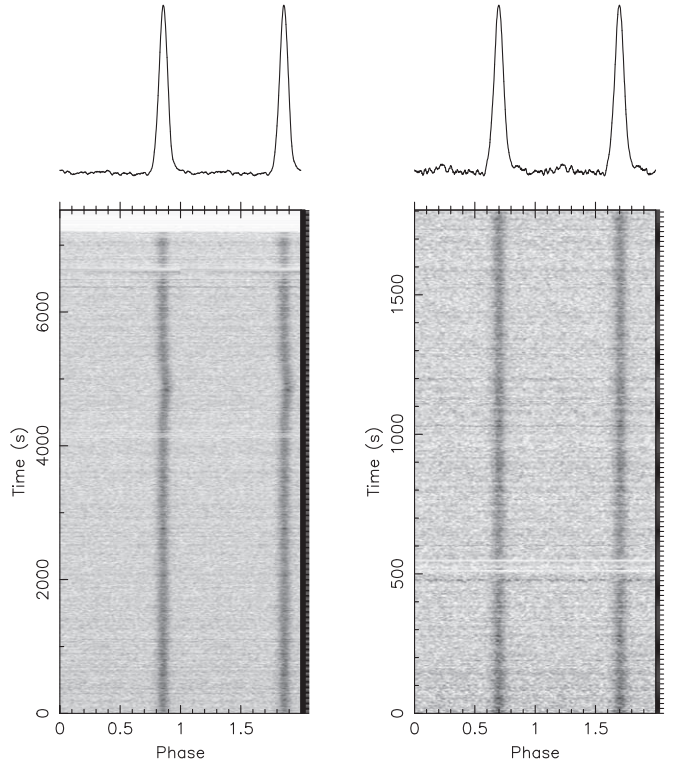

Figure 2. Phase–time (bottom) and integrated profile (top) plots for PSR J1853–0842A obtained with observation data on MJD 58,685 (left) and 58,768 (right).

about 50 pulsars obtained with the Very Long Baseline Array (VLBA) to those predicted by the NE2001 (Cordes & Lazio 2002) and YMW16 (Yao et al. 2017) Galactic electron density distribution models show that it is hard to give a definite conclusion on which model is more accurate. Both models show large errors for some objects, with the NE2001 model doing better on some objects and the YMW16 model on others. For about 14% of those 50 pulsars, their distances based on the YMW16 model fall outside the range of 0.1–1.9 times of corresponding real results obtained with the VLBA (Deller et al. 2019). The Galactic longitude and latitude of NGC 6712 are 25°.35 and −4°.32, respectively. We have limited information about spiral arms and the Scutum stellar cloud along this direction. There is only one pulsar that has a model-independent distance measurement result within 5° around NGC 6712. As we do not know which Galactic electron density model is more accurate, we give a statistic on $D_{\rm YMW16}$ and $D_{\rm NE2001}$ of 87 pulsars within 5° around NGC 6712. The distances of these pulsars are obtained from the pulsar catalog (PSRCAT; Manchester et al. 2005).[16] Figure 3 shows the $D_{\rm YMW16}/D_{\rm NE2001}$ ratios of these 87 pulsars change with $D_{\rm YMW16}$. It is clear the ratio gets larger as the $D_{\rm YMW16}$ gets farther away. When the $D_{\rm YMW16}$ is larger than 6.0 kpc, the ratio can get as large as more than 2.5 times. So the association between PSR J1853–0842A and NGC 6712 cannot simply be excluded based on their large model-dependent distance differences mentioned above because of their unknown accuracy.

The rotation of a pulsar usually slows down with time, as its rotational energy is converted to radiation power. So the

[16] http://www.atnf.csiro.au/research/pulsar/psrcat

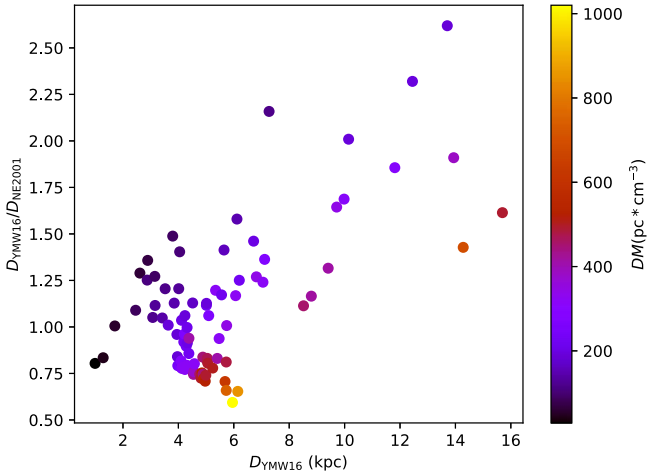

Figure 3. $D_{\rm YMW16}/D_{\rm NE2001}$ changes with $D_{\rm YMW16}$ for 87 pulsars within 5° around NGC 6712. The DM value of each pulsar is scaled with the color bar on the right.

intrinsic spin-down rate ($\dot{P}_{\rm int}$) ought to be a positive value. But the observed spin-down rate ($\dot{P}_{\rm obs}$) of PSR J1853–0842A is about -2.39×10^{-21} s s^{-1}, which is a negative result. The $\dot{P}_{\rm int}$ of a pulsar (especially MSP) is usually contaminated by acceleration of the host Galaxy (a_G) and the Shklovskii effect caused by its proper motion (Shklovskii 1970). In addition, the acceleration effect of the host GC (a_L) should also be considered as it sometimes gives the dominant contribution to the $\dot{P}_{\rm obs}$ of the pulsar in the GC. According to Phinney (1993),

$$\dot{P}_{\rm obs}=\dot{P}_{\rm int}+\frac{a_G}{c}P+\frac{V_\perp^2}{cD}P+\frac{a_L}{c}P, \tag{2}$$

where P is the observed pulsar period, $V_\perp^2/cD$ is the Shklovskii effect, $V_\perp$ is the transverse velocity, D is the distance to the pulsar, and c is the speed of light. We assume the Galaxy has a flat rotation curve in the region of interest, with the Galactocentric distance of the Sun $R_0=8.0$ kpc and rotation velocity $\Theta_0=220$ km s^{-1} (Reid 1993). A straightforward geometric analysis gives the line-of-sight acceleration between the Sun and a pulsar at distance D and Galactic coordinates l and b as follows:

$$a_G=-\cos b\left(\frac{\Theta_0^2}{R_0}\right)\left(\cos l+\frac{\beta}{\sin^2 l+\beta^2}\right), \tag{3}$$

where $\beta=(D/R_0)\cos b-\cos l$ (Damour & Taylor 1991). In the Shklovskii effect calculation, we use $V_\perp=85$ km s^{-1}, which is the average velocity of MSPs (Toscano et al. 1999), as the velocity of PSR J1853–0842A was not fitted successfully with our observation data. If PSR J1853–0842A lies outside the NGC 6712 at a distance of 4.4 kpc (the average DM-based distances are listed in Table 2), the a_G/cP and $V_\perp^2P/(cD)$ are 3.81×10^{-22} and 3.42×10^{-22} s s^{-1}, respectively. Taking $\dot{P}_{\rm int}>0$ and $a_L/cP=0$ into consideration, it is impossible to obtain $\dot{P}_{\rm obs}=-2.39\times10^{-21}$ as all the terms on the right side of Equation (2) are no less than 0. On the other hand, if PSR J1853–0842A is located in NGC 6712 at a distance of 6.9 kpc, a_G/cP and $V_\perp^2P/(cD)$ are 2.43×10^{-22} and -9.35×10^{-22} s s^{-1}, respectively, with the same assumption of

$V_\perp = 85\,\mathrm{km\,s^{-1}}$. Compared with the core position of NGC 6712 and PSR J1853–0842A listed in Tables 1 and 2, it is clear that the pulsar's projected distance from the center of the GC ($R_{\rm psr}$) is less than 2 times that of its core radius (R_c). Under this condition, the maximum acceleration effect of GC can be estimated within 10% of accuracy with the equations:

$$\frac{a_{\rm L,\,max}}{c} \approx \frac{3\sigma_{\rm v}^2}{2c(R_c^2 + R_{\rm psr}^2)^{1/2}}, \quad (4)$$

where σ_v is the central velocity dispersion (Phinney 1993). For PSR J1853–0842A, $a_{\rm L,\,max}/cP$ is about $1.28 \times 10^{-20}\,\mathrm{s\,s^{-1}}$. Though we do not currently know the three-dimensional position of PSR J1853–0842A in NGC 6712, its real a_L/cP is a certain value in the range of -1.28×10^{-20} to $1.28 \times 10^{-20}\,\mathrm{s\,s^{-1}}$. Accordingly, we give an upper limit of its intrinsic spin-down rate $\dot{P}_{\rm int,\,max} = 1.11 \times 10^{-20}\,\mathrm{s\,s^{-1}}$. It is a reasonable value judging by the $\dot{P}$ measure results of some other BWs. Taking PSRs B1957+20 and J2051−0827, for example, their $\dot{P}$ are 2.7×10^{-20} and $1.27 \times 10^{-20}\,\mathrm{s\,s^{-1}}$, respectively (Arzoumanian et al. 1994; Shaifullah et al. 2016).

Using the orbital period P_b and the projected semimajor axis x_p of the pulsar orbit, the mass function

$$f(M_p, M_c) = \frac{4\pi^2}{G}\frac{x_p^3}{P_b^2} = \frac{(M_c \sin i)^3}{(M_p + M_c)^2}, \quad (5)$$

where G is the gravitational constant, M_p is the mass of the pulsar, M_c is the mass of companion star, and i is the inclination of the binary orbit. Though PSR J1853–0842A is a short P_b binary, it is very hard to determine the mass of each star by measuring post-Keplerian parameters with pulsar timing because of its weak general relativity effects. As the M_p and i of this binary cannot be measured with our observation data, we estimate M_c under some assumptions. According to previous studies, the mass of a radio pulsar predominantly falls in a remarkably narrow mass range $1.38^{-0.06}_{+0.10} M_\odot$ (Thorsett & Chakrabarty 1999). The canonical value of a $1.4\,M_\odot$ pulsar is usually used in most cases. But there are some exceptions, such as PSR J1918-0642 with an extremely low mass of $1.18\,M_\odot$ (Fonseca et al. 2016) and PSR J0740+6620 with extremely high mass of $2.14\,M_\odot$ (Cromartie et al. 2020). Taking these into consideration, further limitations on the M_c are given by assuming the M_p to be 1.0, 1.4, and $2.2\,M_\odot$, respectively. The curves of M_c changing with i and M_p are presented in Figure 4. As the eclipse takes place in PSR J1853–0842A, its inclination angle i must be greater than 60°. We calculate $M_{c,60^\circ}$ for the different assumptions of the M_p and list related results in the second column of Table 3. Lower limits of the companion mass ($M_{c,90^\circ}$) are obtained by assuming an edge-on orbit ($i = 90^\circ$). The corresponding results of $M_{c,90^\circ}$ values are present in the third column of Table 3. The Roche lobe for the companion star of PSR J1853–0842A is calculated by the equation

$$R_L = \frac{0.49aq^{2/3}}{0.6q^{2/3} + \ln(1 + q^{1/3})}, \quad (6)$$

where $q = M_c/M_p$ and a is the separation between the pulsar and its companion (Eggleton 1983). The related results for different M_p and i are present in the fourth (for $i = 60^\circ$) and fifth (for $i = 90^\circ$) columns of Table 3.

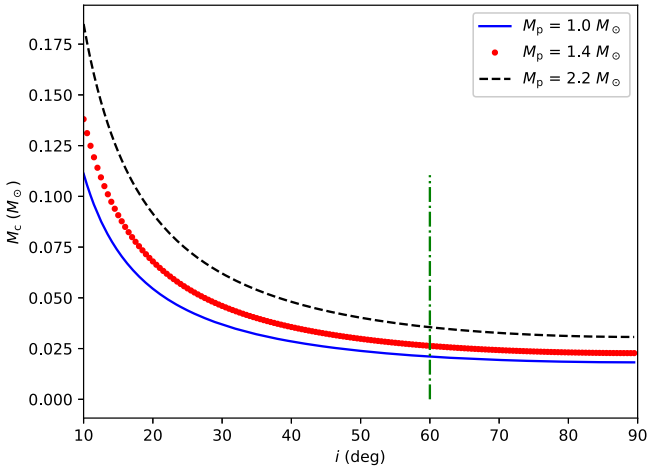

Figure 4. M_c as a function of i and M_p. The case for the assumptions $M_p = 1.0\,M_\odot$, $M_p = 1.4\,M_\odot$, and $M_p = 2.2\,M_\odot$ is shown with solid, dotted, and dashed curves, respectively. The dashed–dotted vertical line stands for $i = 60^\circ$.

Table 3
The Results of M_c, R_L, and R_e for Different i and M_p

M_p ($M_\odot$)	M_c ($M_\odot$)		R_L ($R_\odot$)		R_e ($R_\odot$)	
	$M_{c,60^\circ}$	$M_{c,90^\circ}$	$R_{L,60^\circ}$	$R_{L,90^\circ}$	$R_{e,60^\circ}$	$R_{e,90^\circ}$
1.0	0.021	0.018	0.140	0.134	0.381	0.330
1.4	0.026	0.023	0.152	0.145	0.427	0.370
2.2	0.036	0.031	0.168	0.160	0.497	0.430

About half of the known BW pulsars show eclipse phenomena in which the radio pulses are completely blocked by companion stars (Guillemot et al. 2019). By comparison, the pulse signals of PSR J1853–0842A are affected by extra time delay, but are not absolutely blocked during the eclipse phase. Based on that the extra time delay lasted for about 10% of its orbit at 1.25 GHz, we estimate the radius of ionized material surrounding its companion star (R_e) for different orbital inclination angles and give the related results in the sixth (for $i = 60^\circ$) and seventh (for $i = 90^\circ$) columns of Table 3. It is clear that R_L is smaller than R_e, which indicates that ionized material fully fills the Roche lobe of the companion star. So the outer material is being blown off the companion by the pulsar. As what is shown in this table, the M_c, R_L, and R_e are within a factor of 2.0, 1.3, and 1.5 of the minimum values, respectively. So we will use the values corresponding to the case of canonical pulsar mass $M_p = 1.4\,M_\odot$ and $i = 90^\circ$ in the following estimation about the properties of eclipse material.

Using the extra delays shown in the timing residual plot in Figure 1, we obtain the corresponding maximum excess DM ($\Delta_{\rm DM}$), which was about 0.028 ± 0.001, 0.036 ± 0.001, and $0.030 \pm 0.002\,\mathrm{pc\,cm^{-3}}$, respectively. The column density of the electron ($N_{e,\,\rm max}$) in the eclipse material was about $9.69 \times 10^{16}\,\mathrm{cm^{-2}}$, estimated with the average $\Delta_{\rm DM}$, which is about 5.7 times larger than that of BW PSR J0023–7203J ($N_{e,\,\rm max} = 1.7 \times 10^{16}\,\mathrm{cm^{-2}}$). The radiations of PSR J0023–7203J also passed the material around the companion at both 660 and 1400 MHz with extra time delays (Freire et al. 2003). The radiations of several BWs are blocked at low radio frequencies, but get passed at higher frequencies

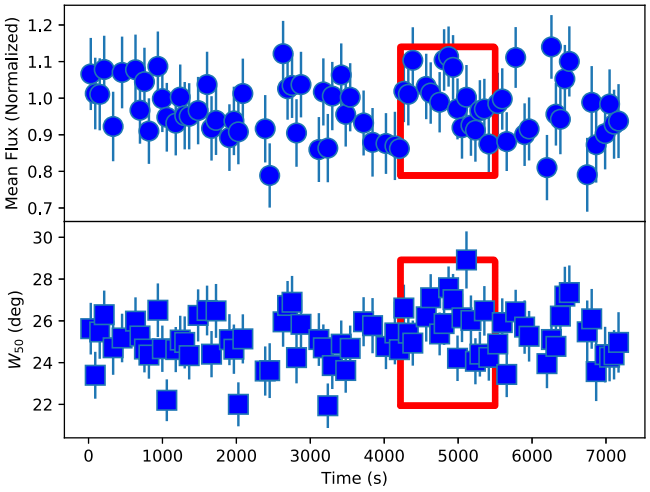

Figure 5. The W_{50} and normalized flux density changed with time for observation on MJD 58,685. The eclipse time range is labeled with the red box.

with extra time delays. PSR J1544+4937 was found to be eclipsing for 13% of its orbit at 322 MHz, whereas the pulsar was detected throughout the low-frequency eclipsing phase at 607 MHz, which was affected by the material around its companion with $N_{e,\,\max} = 8 \times 10^{16}\,\mathrm{cm}^{-2}$ (Bhattacharyya et al. 2013). The material with $N_{e,\,\max} \sim 10^{17}\,\mathrm{cm}^{-2}$ surrounding BW PSR J2051−0827's companion was also found to be opaque for radiations at 436 and 660 MHz, but transparent at 1.4 GHz (Stappers et al. 1996). By comparison, the $N_{e,\max}$ near the superior conjunction of BW PSR J2055+3829 was no less than $10^{17}\,\mathrm{cm}^{-2}$, which was larger than that of the BWs mentioned above. And its radiation was found to be blocked at 1.4 GHz in the eclipse phase (Guillemot et al. 2019). Judging from the information mentioned above, we infer that the radiation of PSR J1853–0842A has the possibility of being blocked at lower radio frequencies.

Graduate flux density decreases (and increases) were detected in PSRs J2051−0827 and J2055+3829 before (and after) their radiations were completely eclipsed at the corresponding frequency (Stappers et al. 1996; Guillemot et al. 2019). For PSR J1853–0842A, we also analyzed its pulse flux density and shape changes with time to investigate how they changed in the eclipse phase. Considering the sensitivity and the time resolution, the W_{50} was used in the pulse shape analysis, and the mean flux normalized with the peak flux density of integrated profile was used to seek its flux variations. Figure 5 shows how these two parameters changed in observation on MJD 58,685, which spanned the longest time and covered the full eclipse phase. No clear change in flux density and W_{50} were found in the eclipse phase compared with the normal state.

Base on the eclipse properties of PSR J1853–0842A, we try to give some constraints on the accretion process of this system. From the results listed in Table 3, it is clear that R_e does not change a lot for different assumptions of i and M_p. Considering only the upper limit of $\dot{P}_{\mathrm{int,max}}$ obtained and eclipse-to-eclipse variability of extra DM delays, we only give rough estimations on the accretion with the average volume density of electron $n_e = 1.88 \times 10^6\,\mathrm{cm}^{-3}$ by assuming $M_p = 1.4 M_\odot$ and $i = 90°$. The energy density of an isotropic pulsar wind at the distance of the companion is given by $U_E = \dot{E}/(4\pi c a^2)$, where $\dot{E} = 4\pi^2 I \dot{P} P^{-3}$ is the spin-down power of the pulsar, I is the moment of inertia, and a is the distance to the companion. For the canonical $1.4\,M_\odot$ neutron star of radius 10 km and moment of inertia $I = 10^{45}\,\mathrm{g\,cm}^2$, the maximum $\dot{E}$ of PSR J1853–0842A is about $4.42 \times 10^{34}\,\mathrm{erg\,s}^{-1}$. If the pulsar wind energy flow is converted into a mass outflow of kinetic energy density with an efficiency factor ϵ, the outflow velocity of ablated material from the companion star

$$V_W \approx \left(\frac{2\epsilon U_E}{n_e m_p}\right)^{1/2}, \tag{7}$$

where n_e and m_p are the electron volume density and proton mass, respectively (Thompson et al. 1994). By assuming $\epsilon = 1$, the upper limit of the mass-loss rate from the companion $\dot{M}_C \simeq \pi R_e^2 m_p n_e V_W$. For PSR J1853–0842A, the corresponding upper limit of $\dot{M}_C$ should be about $3.05 \times 10^{-13}\,M_\odot\,\mathrm{yr}^{-1}$. By comparison, the $\dot{M}_C$ of PSR J1810+1744 are $6 \times 10^{-13}\,M_\odot\,\mathrm{yr}^{-1}$ and $1 \times 10^{-12}\,M_\odot\,\mathrm{yr}^{-1}$, using the observations at 149 MHz and 345 MHz, respectively (Polzin et al. 2018). The inferred accretion rates of these two BWs are comparable.

Overall, the newly discovered BW pulsar J1853–0842A is most probably in NGC 6712. During the eclipse phase, its signals showed eclipse-to-eclipse varying extra time delays but were not blocked. The average $N_{e,\,\max}$ of material around J1853–0842A's companion is about $9.69 \times 10^{16}\,\mathrm{cm}^{-2}$, which is a medium value compared with BWs that show only extra time delays and absolutely blocked phenomena in the eclipse phase. Its inferred upper limit of $\dot{M}_C$ of about $3.05 \times 10^{-13}\,M_\odot\,\mathrm{yr}^{-1}$ is also comparable with some other BWs. We predict that the radiation of PSR J1853–0842A has the possibility of being blocked at lower radio frequencies, and will test this hypothesis with future observations.

We would like to express our appreciation to the anonymous reviewer and Professor R. N. Manchester for their good suggestions. This work was supported in part by the National Natural Science Foundation of China (grant Nos. U2031119, U1631122, 12041301, 11988101, 11703047, 11773041, 11633007, and 11403073), the Strategic Priority Research Program of the Chinese Academy of Sciences (XDB23010200), the National Key R&D Program of China (2018YFA0404602), and the Knowledge Innovation Program of the Chinese Academy of Sciences (KJCX1-YW-18). Z.P. is supported by the CAS "Light of West China" Program. Five-hundred-meter Aperture Spherical radio Telescope (FAST) is a National Major Scientific Project built by the Chinese Academy of Sciences. Funding for the project has been provided by the National Development and Reform Commission. FAST is operated and managed by the National Astronomical Observatories, Chinese Academy of Sciences.

ORCID iDs

Zhen Yan https://orcid.org/0000-0002-9322-9319
Zhi-chen Pan https://orcid.org/0000-0001-7771-2864
Scott M. Ransom https://orcid.org/0000-0001-5799-9714
Duncan R. Lorimer https://orcid.org/0000-0003-1301-966X
Lei Qian https://orcid.org/0000-0003-0597-0957
Zhi-qiang Shen https://orcid.org/0000-0003-3540-8746
Di Li https://orcid.org/0000-0003-3010-7661

References

Andersen, B. C., & Ransom, S. M. 2018, ApJL, 863, L13
Archibald, A. M., Stairs, I. H., Ransom, S. M., et al. 2009, Sci, 324, 1411
Arzoumanian, Z., Fruchter, A. S., & Taylor, J. H. 1994, ApJL, 426, L85
Bhattacharyya, B., Roy, J., Ray, P. S., et al. 2013, ApJL, 773, L12
Biggs, J. D., & Lyne, A. G. 1996, MNRAS, 282, 691
Cordes, J. M., & Lazio, T. J. W. 2002, arXiv:astro-ph/0207156
Cromartie, H. T., Fonseca, E., Ransom, S. M., et al. 2020, NatAs, 4, 72
Damour, T., & Taylor, J. H. 1991, ApJ, 366, 501
Deller, A. T., Goss, W. M., Brisken, W. F., et al. 2019, ApJ, 875, 100
Eggleton, P. P. 1983, ApJ, 268, 368
Fonseca, E., Pennucci, T. T., Ellis, J. A., et al. 2016, ApJ, 832, 167
Freire, P. C., Camilo, F., Kramer, M., et al. 2003, MNRAS, 340, 1359
Freire, P. C., Kramer, M., & Lyne, A. G. 2001, MNRAS, 322, 885
Freire, P. C. C. 2013, in IAU Sym. 291, Neutron Stars and Pulsars: Challenges and Opportunities after 80 yr, ed. J. van Leeuwen (Cambridge: Cambridge Univ. Press), 243
Fruchter, A. S., Stinebring, D. R., & Taylor, J. H. 1988, Natur, 333, 237
Fuhrmann, K. 2004, AN, 325, 3
Guillemot, L., Octau, F., Cognard, I., et al. 2019, A&A, 629, A92
Harris, W. E. 1996, AJ, 112, 1487
Hui, C. Y., Cheng, K. S., & Taam, R. E. 2010, ApJ, 714, 1149
Jiang, P., Tang, N.-Y., Hou, L.-G., et al. 2020, RAA, 20, 064
Jiang, P., Yue, Y., Gan, H., et al. 2019, SCPMA, 62, 959502
Leahy, D. A., Darbro, W., Elsner, R. F., et al. 1983, ApJ, 266, 160
Lorimer, D. R., & Kramer, M. 2004, Handbook of Pulsar Astronomy, Vol. 4 (Cambridge: Cambridge Univ. Press)
Lynch, R. S., Ransom, S. M., Freire, P. C. C., & Stairs, I. H. 2011, ApJ, 734, 89
Lyne, A. G., Brinklow, A., Middleditch, J., Kulkarni, S. R., & Backer, D. C. 1987, Natur, 328, 399
Manchester, R. N., Hobbs, G. B., Teoh, A., & Hobbs, M. 2005, AJ, 129, 1993
Nan, R. 2006, ScChG, 49, 129
Nan, R., Li, D., Jin, C., et al. 2011, IJMPD, 20, 989
Nice, D., Demorest, P., Stairs, I., et al. 2015, Tempo: Pulsar timing data analysis, Astrophysics Source Code Library, ascl:1509.002
Ortolani, S., Momany, Y., Barbuy, B., Bica, E., & Catelan, M. 2000, A&A, 362, 953
Phinney, E. S. 1993, in ASP Conf. Ser. 50, Structure and Dynamics of Globular Clusters, ed. S. G. Djorgovski & G. Meylan (San Francisco, CA: ASP), 141
Polzin, E. J., Breton, R. P., Clarke, A. O., et al. 2018, MNRAS, 476, 1968
Polzin, E. J., Breton, R. P., Stappers, B. W., et al. 2019, MNRAS, 490, 889
Pooley, D., Lewin, W. H. G., Anderson, S. F., et al. 2003, ApJL, 591, L131
Qian, L., Yao, R., Sun, J., et al. 2020, Innov, 1, 100053
Ransom, S. 2011, PRESTO: PulsaR Exploration and Search TOolkit, Astrophysics Source Code Library, ascl:1107.017
Ransom, S. M. 2008, in AIP Conf. Ser. 983, 40 Years of Pulsars: Millisecond Pulsars, Magnetars and More, ed. C. Bassa et al. (Melville, NY: AIP), 415
Ransom, S. M., Eikenberry, S. S., & Middleditch, J. 2002, AJ, 124, 1788
Reid, M. J. 1993, ARA&A, 31, 345
Roberts, M. S. E. 2013, in IAU Symp. 291, Neutron Stars and Pulsars: Challenges and Opportunities after 80 yr, ed. J. van Leeuwen (Cambridge: Cambridge Univ. Press), 127
Ruderman, M., Shaham, J., & Tavani, M. 1989, ApJ, 336, 507
Sandage, A., & Smith, L. L. 1966, ApJ, 144, 886
Shaifullah, G., Verbiest, J. P. W., Freire, P. C. C., et al. 2016, MNRAS, 462, 1029
Shklovskii, I. S. 1970, SvA, 13, 562
Stappers, B. W., Bailes, M., Lyne, A. G., et al. 1996, ApJL, 465, L119
Taylor, J. H. 1992, RSPTA, 341, 117
Taylor, J. H., & Cordes, J. M. 1993, ApJ, 411, 674
Thompson, C., Blandford, R. D., Evans, C. R., & Phinney, E. S. 1994, ApJ, 422, 304
Thorsett, S. E., & Chakrabarty, D. 1999, ApJ, 512, 288
Toscano, M., Sandhu, J. S., Bailes, M., et al. 1999, MNRAS, 307, 925
Turk, P. J., & Lorimer, D. R. 2013, MNRAS, 436, 3720
Verbunt, F., & Hut, P. 1987, in IAU Symp. 125, The Origin and Evolution of Neutron Stars, ed. D. J. Helfand & J.-H. Huang (Dordrecht: Reidel), 187
Webbink, R. F. 1985, in IAU Symp. 113, Dynamics of Star Clusters, ed. J. Goodman & P. Hut (Dordrecht: Reidel), 541
Yao, J. M., Manchester, R. N., & Wang, N. 2017, ApJ, 835, 29